



Continuous detonation of a hydrogen–oxygen gas mixture in a 100-mm plane-radial combustor with exhaustion toward the periphery

F. A. Bykovskii¹ · S. A. Zhdan¹ · E. F. Vedernikov¹ · A. E. Tarnaikin¹ · A. N. Samsonov¹

Received: 9 October 2018 / Revised: 11 June 2019 / Accepted: 21 August 2019 / Published online: 3 September 2019
© Springer-Verlag GmbH Germany, part of Springer Nature 2019

Abstract

Regimes of continuous spin detonation and continuous multifront detonation in a hydrogen–oxygen mixture are obtained in a plane-radial combustor with an inner diameter of 100 mm and exhaustion toward the periphery. The fuel-lean limits of detonation in terms of the specific flow rate of the mixture are determined. For continuous spin detonation, transverse detonation waves and the flow in their vicinity in the combustor plane are reconstructed. The detonation wave is found to be significantly curved because of the increase in the tangential component of the velocity along the combustor radius. It is demonstrated that the scale effect is manifested only in the number of rotating waves. However, their velocity increases with increasing the combustor size. The velocity deficit of continuous detonation is 20–40% as compared to the velocity of the ideal Chapman–Jouguet detonation. (The smaller value corresponds to the fuel-lean mixture.)

Keywords Continuous spin detonation · Plane-radial combustor · Hydrogen–oxygen mixture · Rotating wave · Scale effect · Pitot probes · Transverse detonation wave · Continuous multifront detonation · High-speed filming

1 Introduction

Continuous spin detonation (CSD) of fuel–air and fuel–oxygen mixtures in annular cylindrical combustors is intensively studied by many researchers. Up to now, investigations in plane-radial combustors (PRC) with exhaustion toward the periphery have been performed only in Russia. The first PRC for detonation combustion designed by Voitsekhovskii [1] was constricted at the exit and operated on a premixed acetylene–oxygen mixture. Investigations in the PRC with separate injection of the fuel and oxidizer and without constriction at the exit were continued at the Lavrentyev Institute of Hydrodynamics of the Siberian Branch of the Russian

Academy of Sciences (LIH SB RAS) [2–4]. In those studies, CSD and pulse detonation (PD) regimes were observed in acetylene–oxygen and hydrogen–oxygen mixtures in a PRC with an inner diameter (injector diameter) of 20 mm and an outer diameter (exhaustion of detonation products) of 40, 60, or 80 mm. In 2005, a patent on rotating detonation engine [5] with combustors of similar geometry was obtained. There is a recent publication of Higashi et al. [6] who obtained detonation regimes in experiments with a hydrogen–air mixture in a PRC connected to a compressor and a turbine.

The goal of the present paper is to obtain and study the structure of detonation waves in a PRC with exhaustion of gaseous hydrogen and oxygen flows toward the periphery and also to check the scale effect; the inner diameter of the combustor is $d_{c1} = 100$ mm, and the outer diameter is varied in the interval $d_{c2} = 120$ –300 mm.

This paper is based on work that was presented at the 11th International Colloquium on Pulsed and Continuous Detonations, St. Petersburg, Russia, September 17–21, 2018.

Communicated by F. Lu and A. Higgins.

✉ A. N. Samsonov
samsalexandr@gmail.com

¹ Lavrentyev Institute of Hydrodynamics, Siberian Branch, Russian Academy of Sciences, Novosibirsk, Russia 630090

2 Combustor and test technique

The experiments were performed in a PRC with an inner diameter $d_{c1} = 100$ mm and exhaustion toward the periphery (I) (Fig. 1). The distance between the flat walls (2) was $\Delta = 5$ or 10 mm. The outer diameter of the annular

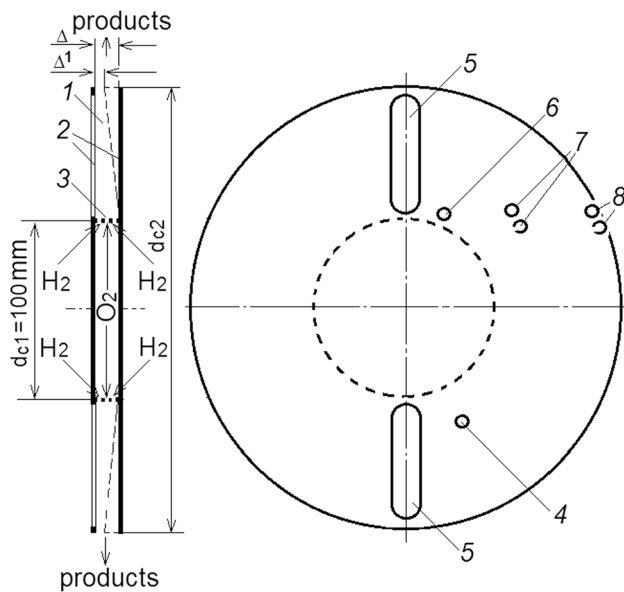


Fig. 1 Schematic of the plane-radial combustor with exhaustion toward the periphery (4—location of the igniter; 5—windows; 6, 7, 8—location of the transducers)

orifice d_{c2} for exhaustion of detonation products was varied: $d_{c2} = 120, 150, 200, \text{ or } 300 \text{ mm}$. The channel length was also varied $L_c = (d_{c2} - d_{c1})/2$. The distance between the flat PRC walls was much smaller than the PRC diameters: $\Delta \ll d_{c1} < d_{c2}$. For the PRC with $d_{c2} = 300 \text{ mm}$ ($\Delta = 10 \text{ mm}$), the channel could be uniformly constricted toward the exit to $\Delta^1 = 3.3 \text{ mm}$ to ensure a constant area of the circular cross section of the channel $S\Delta = 31.4 \text{ cm}^2$.

Separate injection of hydrogen and oxygen into the PRC toward the periphery was performed through injectors (3) uniformly distributed over the circumference on the cylindrical wall and generating a system of intersecting jets to provide mixing of the species near this wall.

The total cross-sectional area of the injectors was $S_f = 34.2 \text{ mm}^2$ for hydrogen and $S_{ox} = 60.8 \text{ mm}^2$ for oxygen. Hydrogen was injected from a receiver with a volume $V_{r,f} = 1.95, 4.2, \text{ and } 10 \text{ L}$; the volume of the oxygen receiver was $V_{r,ox} = 4.2 \text{ or } 1.95 \text{ L}$ (not shown in the figure). The initial pressure was $p_{r,f0} = (30\text{--}48) \times 10^5 \text{ Pa}$ in the hydrogen receivers and $p_{r,ox0} = (30\text{--}52) \times 10^5 \text{ Pa}$ in the oxygen receivers. The initial flow rates of the $\text{H}_2\text{--O}_2$ mixture varied in the following ranges: $G_{f0} = 31.2\text{--}90.1 \text{ g/s}$ (hydrogen) and $G_{ox0} = 363\text{--}576 \text{ g/s}$ (oxygen).

The current flow rates of the gases were determined on the basis of pressure reduction in the oxygen and hydrogen receivers ($p_{r,ox}$ and $p_{r,f}$) [7]. The specific flow rate of the mixture was $g_\Sigma = (G_f + G_{ox})/S\Delta = 13.7\text{--}336 \text{ kg/(s m}^2)$, and the fuel-to-oxidizer equivalence ratio was $\phi = 0.26\text{--}1.7$. Here $S\Delta = \pi d_{c1} \cdot \Delta$ is the area of the PRC entrance.

The process was initiated near the flat wall at a distance of 20 mm from the PRC (4) entrance by blasting an aluminum foil strip by electric current (the energy release was approximately 1 J). The method for determining the magnitude of the discharge energy was described in detail in [8]. The initiation system triggering was synchronized with injection of oxygen into the combustor, which took place behind hydrogen injection. The combustion products escaped into the atmosphere with the ambient pressure $p_a = 1.0 \times 10^5 \text{ Pa}$. The process was observed through two Plexiglas windows 95 mm long and 10 mm wide (5) (see Fig. 1), which were mounted in the radial direction on one of the flat walls of the combustor and covered almost the entire flow field. It was only a small flow region near the injectors (at a distance of 5 mm) that could not be visualized. The flow along the windows was illuminated by thin acetylene filaments injected exactly in this blind part of the channel.

The process in the PRC was photographed by a Photron FASTCAM SA5 high-speed camera with a frequency of 420,000 or 620,000 frames per second. The exposure time of the high-speed videos was 2.4 or 1.6 microseconds. Based on the frames scanned along the windows, a special computer code was applied to choose a line with a width of one pixel, which was then combined with similar lines from other frames. As a result, we obtained a complete pattern of the flow in the wave-fixed system. The luminescent objects moving in the tangential direction were detected with some distortions because they moved over circumferences of different diameters. Processing the frames obtained by scanning across the window, we obtained a (x, t) diagram of detonation waves and products moving over the circumference. The photographic records and the (x, t) diagrams were used for finding the time Δt when the detonation waves arrived opposite the window, which allowed determination of their frequency f :

$$f = 1/\Delta t.$$

In the case of CSD, it was also possible to calculate the velocity D of the motion of transverse detonation waves (TDWs) with respect to the cylindrical surface diameter d_{c1} :

$$D = \pi \cdot d_{c1}/(n \cdot \Delta t).$$

Here n is the number of TDWs along the combustor circumference.

The following pressure measurements were performed: pressures in the hydrogen ($p_{r,f}$) and oxygen ($p_{r,ox}$) receivers, pressures in the corresponding manifolds ($p_{m,f}$ and $p_{m,ox}$), static pressures p_{c1} in the combustor at a distance of 10 mm from the cylindrical surface (6), static (p_{c2}) and total (p_{c20}) pressures (with the use of the pitot probes) at a distance of 50 mm from the cylindrical surface (7), and static (p_{c3}) and total (p_{c30}) pressures at the PRC exit (8) (see Fig. 1). The pressure measurements were performed by certified

pressure probes with the accuracy class of 0.5% produced by the Trafag company (Switzerland).

3 Experimental results

3.1 Combustor with $\Delta = 10$ mm and $d_{c2} = 300$ mm

Regimes of continuous spin detonation and continuous multifront detonation (CMD) with opposing TDWs [9] were obtained in the ranges of the specific flow rates of the mixture $\text{H}_2\text{-O}_2$ $g_{\Sigma} = 27\text{--}208$ kg/(s m²) and the fuel-to-oxidizer equivalence ratios $\phi = 0.48\text{--}1.53$. Two typical fragments of photographic records are illustrated in Fig. 2a, b.

The duration of the fragments of the process along the band of the photographic record is 2.1 ms (left) and 0.16 ms (right, more detailed fragments, highlighted in the white frame). As the pictures were taken through two windows, two bands of detonation waves were recorded for each regime. These bands are separated by a dark bar at the center of the picture, which is the nearest distance between the windows along the combustor diameter: $d_{c1} + 2 \times 5$ mm = 110 mm, where 5 mm

is the distance from the PRC entrance to the edge of the window. This dark bar serves as a scale of the photographic records. In reconstructing the flow in the wave-fitted system by the above-mentioned special computer code, the wave rotation direction was not determined; only those luminescent points that consecutively pass opposite the window were detected. Therefore, it seems that the waves in the photographic records are aligned in the same direction, whereas in fact the waves in the upper and lower windows have opposite orientations despite an identical tangential direction of wave rotation. Therefore, each point, e.g., in the upper window, should have its mirror reflection with respect to the vertical axis.

Figure 2a (left) shows the instant of initiation (bright flash) and further evolution of the detonation process. TDWs moving in one direction start to develop approximately for 0.5 ms, but then the process transforms to the CMD regime. The detonation and shock waves and also the flow in the vicinity of these waves are clearly seen in a small fragment (Fig. 2a, right). By analogy with the structure of the classical multifront detonation of gaseous explosive mixtures [10], one can assume that the velocities of the detonation

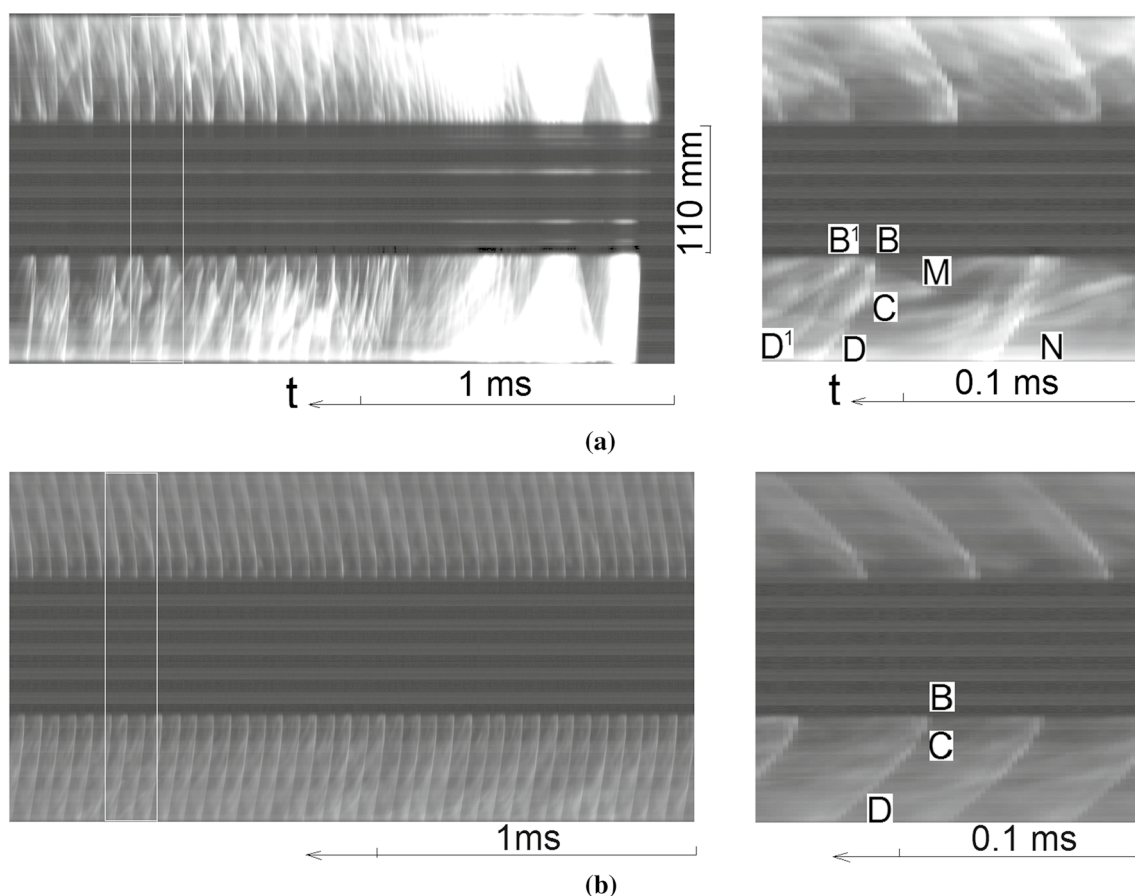


Fig. 2 Typical photographic records (fragments) for $\Delta = 10$ mm, $d_{c2} = 300$ mm: **a** CMD, $g_{\Sigma} = 157$ kg/(s m²), $\phi = 1.51$, and $f = 19.3$ kHz; **b** CSD, $g_{\Sigma} = 87$ kg/(s m²), $\phi = 0.85$, $n = 3$, $f = 18.4$ kHz, and $D = 1.93$ km/s

wave front **BC** of height $h \approx 35$ mm and the adjacent tail **CD** increase up to the maximum value before the impact. The TDW front height is counted from the cylindrical surface (point B) to its intersection with the contact surface between the fresh mixture and reaction products (point C). After the “forward” TDW collides with the “opposing” TDW (outside the frame), it degenerates into a shock wave **B¹D¹** and moves in the opposite direction, first over the detonation products away from the forward wave and then with a growing velocity over the mixture layer, increasing until the instant of the next collision at another point. The same occurs for the “opposing” TDW. The process is extremely irregular in terms of both the TDW structure and the flow near the TDW. In this case, one can talk about the frequency f , but hardly about the mean detonation velocity, because it is difficult to identify the number of waves on the combustor circumference. As the products move in an expanding channel (at $\Delta = \text{const}$) and escape into a medium with the ambient pressure $p_a = 1.0 \times 10^5$ Pa, for a comparatively moderate total pressure at the PRC entrance $p_0 = (D_{CJ}/\gamma) \cdot g_\Sigma = 3.9 \times 10^5$ Pa [7], the supersonic flow of the products is decelerated in shock waves MN, which penetrate into the PRC up to its entrance. Here $D_{CJ} = 3.1$ km/s is the velocity of the ideal Chapman–Jouguet detonation for $\phi = 1.51$ [11], $\gamma \approx 1.25$ is the effective ratio of specific heats of the products [12], and $g_\Sigma = 157$ kg/(s m²).

As the specific flow rate of the mixture decreases, the CMD regime with opposing TDWs persists down to $g_\Sigma = 105$ kg/(s m²) and then transforms to the regular CSD regime (Fig. 2b). The layer of the mixture ahead of the front BC is sufficiently stable ($h \approx 15$ mm); relative to the distance to the next wave l , the ratio is $h/l \approx 1/7$. In annular cylindrical combustors with channel expansion, this ratio has greater values: $h/l \approx 1/5$ [7]. In the intervals $g_\Sigma = 105 \rightarrow 50$ kg/(s m²) and $\phi = 1.01 \rightarrow 0.54$, three ($n = 3$) TDWs with velocities $D = 1.93 \rightarrow 1.99 \rightarrow 1.89$ km/s ($f = 18.4 \rightarrow 19 \rightarrow 18$ kHz) propagate in the PRC; then, a fourth wave is formed as $g_\Sigma = 50 \rightarrow 43.3$ kg/(s m²) and $\phi = 0.54 \rightarrow 0.5$, and the TDW velocity decreases to $D = 1.52$ km/s ($f = 19.4$ kHz). The arrow indicates the direction of the change in parameter during the experiment. The observed oscillations of the TDW velocity and the increase in the number of waves are apparently

associated with the decrease in the pressure in the combustor and deeper penetration of MN-type shock waves (see Fig. 2a) inward of the combustor. Acoustic waves are observed at $g_\Sigma < 43.3$ kg/(s m²). If the number of waves rotating in the combustor is known, it is possible to scale the fragment of the photographic records in Fig. 2b (left) with respect to the diameter of the cylindrical surface of the combustor (Fig. 2b, right). As the photographic record of the process is linear, the fragment recorded through one of the windows (lower window in the case considered here) should be rolled into a ring for obtaining the real pattern of the flow in the combustor. The fragment in Fig. 2a (right) cannot be rolled into a ring because the process is unsteady: The recorded wave structures and the flow structures in the vicinity of these waves are essentially different in the upper and lower windows. A detailed flow pattern can be captured by performing frame-by-frame recording of the entire process through a transparent wall, as it was done in [13].

The values of the process parameters in a plane-radial combustor with $\Delta = 10$ mm for several experiments are listed in Table 1. It should be noted that combustion with acoustic waves is observed in the combustor for the values of g_Σ smaller than those given in Table 1.

Figure 3a, b shows the pressure oscillograms in the injection system and PRC during the experiment whose photographic records (fragments) are presented in Fig. 2.

It is seen that the pressure $p_{r,f}$ in the hydrogen receiver decreases faster during the experiment than the pressure $p_{r,ox}$ in the oxygen receiver. Therefore, the fuel-to-oxidizer equivalence ratio ϕ decreases: $\phi = 1.51 \rightarrow 0.4$. The flow of the products near the sensors (p_{c2}) and p_{c20} is supercritical approximately at the time of changing of the CMD to CSD mode (line 3). At the PRC exit, the pressure shock moves from outside into the channel, the flow turns to the subcritical state, and the total pressure p_{c30} becomes almost equal to the static pressure p_{c3} (Fig. 3b). Significant pressure oscillations caused by detonation waves around their average values are detected in the PRC, but these are not true values of the pressure amplitude in the PRC because of the inertia of the sensors. The injection pressures are sufficiently high to ensure the necessary flow rates of the mixture components; therefore, the processes

Table 1 Parameters of CMD and CSD in the combustor with $\Delta = 10$ mm

L_c , mm	g_Σ , kg/(s m ²)	ϕ	f , kHz	n	D , km/s	p_{c1}/p_a	Regime
100	157 → 105	1.51 → 1.01	19.3 → 14.9	–	–	1.83 → 1.3	CMD
	105 → 43.3	1.01 → 0.5	18.4 → 19.4	3 → 4	1.93 → 1.52	1.3 → 1.0	CSD
100 ($\Delta^1 = 3.3$ mm)	163 → 45	1.39 → 0.5	53.2 → 23.9	8 → 5	2.09 → 1.5	3.7 → 1.1	CSD
50	155 → 115	1.53 → 1.14	13.5 → 16.5	–	–	1.9 → 1.51	CMD
	115 → 43	1.14 → 0.48	20.8 → 18.5	3 → 4	2.0 → 1.45	1.51 → 1.0	CSD
50	208 → 108	1.08 → 0.99	35.6 → 21.8	–	–	2.5 → 1.4	CMD
	108 → 27	0.99 → 0.85	18.7 → 27	3 → 6	1.96 → 1.4	1.4 → 0.97	CSD

in the combustor do not produce any significant effect on the injection system.

As the PRC channel is constricted from $\Delta = 10$ to $\Delta^1 = 3.3$ mm (see Fig. 1), the conditions in the combustor and the detonation process become essentially different. The static pressure in the combustor is approximately doubled at the critical exhaustion of the products. Continuous spin detonation is observed in the intervals $g_{\Sigma} = 163 \rightarrow 45$ kg/(s m²) and $\phi = 1.39 \rightarrow 0.5$ (see Table 1). The mixture burns in a greater number of TDWs ($n = 8 \rightarrow 5$) with TDW velocities $D = 2.09 \rightarrow 1.5$ km/s. The wave velocities and the number

of waves were cross-checked on the basis of (x, t) diagrams of repeated experiments for the same initial conditions. The TDW structure and the (x, t) diagrams are similar to those shown in Figs. 4 and 5 (the left part of the records), respectively.

3.2 Combustor with $\Delta = 10$ mm and $d_{c2} = 200$ mm

The experiments were aimed at minimizing the PRC length L_c (outer diameter d_{c2}). It is seen in Fig. 2b that the detonation front BC is rather small ($h \approx 15$ mm) as compared to the

Fig. 3 Pressure oscillograms in **a** the injection system and **b** PRC; 1—initiation (fragment in Fig. 2a), 2—pressures corresponding to the fragment in Fig. 2b, 3—boundary between the CMD and CSD processes

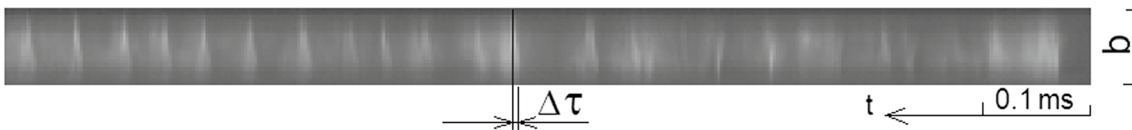
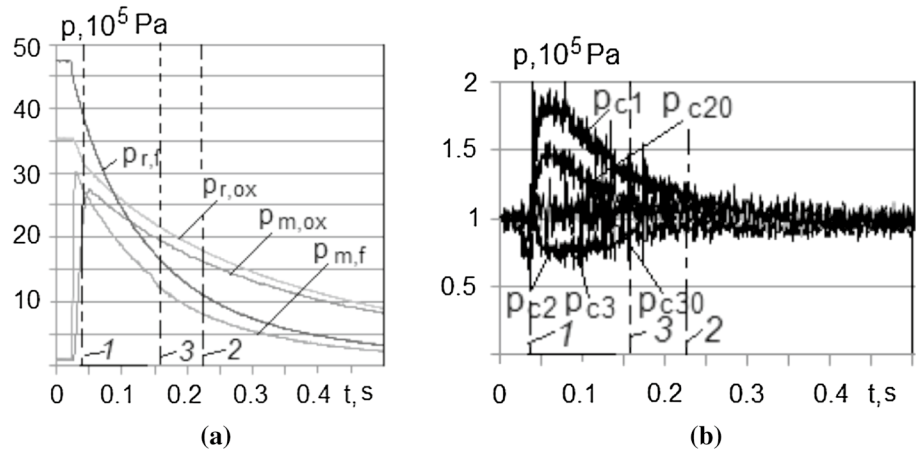


Fig. 4 (x, t) diagram illustrating the CMD transformation to CSD for $\Delta = 10$ mm, $d_{c2} = 200$ mm: $g_{\Sigma} = 114$ kg/(s m²), $\phi = 0.99$; CMD— $f = 13.8$ kHz; CSD— $f = 24.9$ kHz, $n = 4$, and $D = 1.96$ km/s

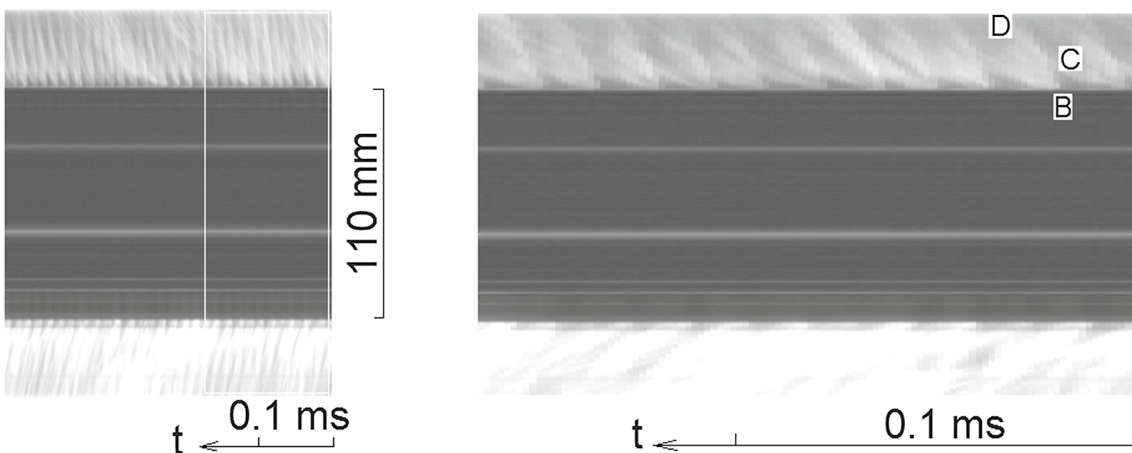


Fig. 5 Typical photographic records (fragments) of CSD in the PRC: $\Delta = 5$ mm, $d_{c2} = 200$ mm; $g_{\Sigma} = 323$ kg/(s m²), $\phi = 1.0$, $f = 68.9$ kHz, $n = 11$, and $D = 1.97$ km/s

PRC channel length $L_c = 100$ mm. Therefore, the streamlines pass through the detonation wave tails **CD** several (4–5) times, which increases the entropy of the products. For this reason, the outer diameter of the combustor was reduced to $d_{c2} = 200$ mm, resulting in approximately twofold reduction in the PRC channel length (to 50 mm). The overall character of the process in the combustor was the same (CMD followed by CSD). The wave structure and the flow in the vicinity of these waves are similar to those presented in Fig. 2 for $d_{c2} = 300$ mm. However, the transformation of the detonation regimes occurred slightly earlier: at $g_{\Sigma} = 115 \pm 5$ kg/(s m²) and $\phi = 1.14$ in one experiment and at $\phi = 1.0$ in another experiment. In the first test, the oxygen and hydrogen receivers had identical volumes: $V_{r,ox} = V_{r,f} = 4.2$ L; therefore, the decrease in the pressure in these receivers during the run was close to that shown in Fig. 3a. In the second case, the oxygen and hydrogen receivers had the volumes $V_{r,ox} = 4.2$ L and $V_{r,f} = 1.95$ L, which allowed to stabilize the fuel-to-oxidizer equivalence ratio during the test. To verify the number of waves, their velocities, and transformation of the detonation regimes, photographs of the flow were also taken across the window ((x, t) diagrams). One of them is shown in Fig. 4. (The instant of CMD transformation to CSD is chosen.)

It is seen that the tangential traces of the moving objects in the right part of the (x, t) diagram exhibit an irregular behavior and are inclined in the opposite directions, which clearly indicates that the waves rotate in different directions and collide with each other (the CMD mode). In the left part of the (x, t) diagram, the photographic records of the moving objects are regular and have identical slopes, which is a clear indication of the CSD mode. Based on the known width of the window ($b = 10$ mm) and time interval ($\Delta\tau$) between the beginning and the end of the photographic record, one can determine the approximate TDW velocity. The number of waves n and the exact TDW velocity are found from the formula $D = \pi \cdot d_{c1} / (n \cdot \Delta t)$.

3.3 Combustor with $\Delta = 5$ mm and $d_{c2} = 120, 150,$ or 200 mm

CSD regimes were obtained in this PRC for all values of the specific flow rate of the H₂–O₂ mixture: $g_{\Sigma} = 13.7$ – 336 kg/(s m²). (The process parameters for several values of d_{c2} obtained in some particular experiments are listed in Table 2.)

The greatest number of TDWs (up to $n = 14$) was observed at large values of g_{Σ} and ϕ . Figure 5 shows the typical photographic records of CSD in the PRC with $\Delta = 5$ mm and $d_{c2} = 200$ mm.

The left part of the figure shows the original photographic record, which is normalized to the real scale (the inner diameter of the combustor with 11 TDWs rotating in the plane of the combustor) on the right. The TDW front height BC is $h \approx 10$ mm ($h/l \approx 1/3$). The TDW front structure, the number of waves, and their velocities were similar for the combustors with $d_{c2} = 120, 150,$ and 200 mm. As the flow rate g_{Σ} decreased during the experiment, the number of waves decreased to three or four. (The velocity was $D = 2.0 \pm 0.2$ km/s.) The TDW front height increased to $h \approx 15$ mm, and the ratio h/l decreased to $h/l \approx 1/7$. In the PRC with $d_{c2} = 120$ mm ($L_c = 10$ mm) and specific flow rate $g_{\Sigma} = 238 \rightarrow 204$ kg/(s m²), the TDW front occupied the entire length of the annular channel along the radius. At $g_{\Sigma} < 238$ kg/(s m²) and reduction in the number of TDWs, more and more mixture went outside the annular gap. The number of waves drastically changed from $n = 10$ to 7 and then to 3. In the interval $g_{\Sigma} = 250$ – 336 kg/(s m²), partial burnout of the mixture was observed in the annular channel, and radial pulse detonation waves with the frequency $f = 5.4$ – 6 kHz were formed at the channel exit, where the unburned remainder of the mixture burned down completely. In the combustor with $d_{c2} = 150$ and 200 mm, the TDW front did not pass outside the PRC as the number of waves decreased.

4 Analysis of results

The CMD regime of detonation burning of hydrogen–oxygen mixtures was obtained for the first time in a combustor with the gap width $\Delta = 10$ mm. This regime was observed previously in the case of burning of an acetylene–oxygen mixture near the cylindrical surface with $d_{c1} = 20$ mm (in a combustor without side walls) [14], ethylene–oxygen mixture in a PRC with exhaustion toward the center [13], and methane/hydrogen–air mixture in an annular cylindrical combustor 503 mm in diameter [9]. The fuel-lean limit of the CMD regime in terms of the specific flow rate of the H₂–O₂ mixture in most experiments was $g_{\Sigma\min} = 100 \pm 15$ kg/(s m²) and $\phi = 0.53$ – 1.0 . The fuel-rich limit was not determined because

Table 2 Parameters of CSD in the combustor with $\Delta = 5$ mm

L_c , mm	g_{Σ} , kg/(s m ²)	ϕ	f , kHz	N	D , km/s	p_{c1}/p_a	Regime
50	323 → 30	1.12 → 0.67	117 → 26	12 → 4	2.3 → 2.14	4.2 → 0.97	CSD
25	292 → 21	1.45 → 0.96	93.3 → 31.8	14 → 5	2.36 → 2.0	4.1 → 1.0	CSD
10	336 → 250	1.3 → 1.0	–	–	–	0.5	Combust.
	250 → 81	1.0 → 0.43	15.6 → 13.8	13 → 3	1.99 → 1.97	3.1 → 0.9	CSD

of the setup capabilities, which could ensure $g_{\Sigma} < 210 \text{ kg}/(\text{s m}^2)$ for $\Delta = 10 \text{ mm}$. However, only CSD regimes were observed in the combustor with $\Delta = 5 \text{ mm}$ for all flow rates in the interval $g_{\Sigma} = 13.7\text{--}336 \text{ kg}/(\text{s m}^2)$. For all values of Δ and L_c , we did not observe pulse detonation (PD) along the radius, which occurred in these intervals of g_{Σ} in the combustor with $d_{c1} = 20 \text{ mm}$. A possible reason is attenuation of centrifugal forces, which favor better mixing near the cylindrical surface and CSD formation.

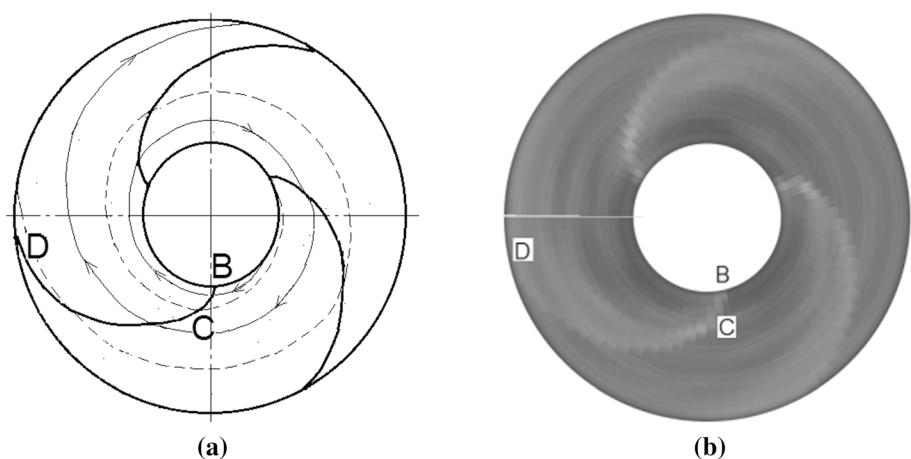
Based on the number of TDWs and their velocity, it is seen that only a partial scale effect is observed in the PRC with exhaustion toward the periphery, in contrast to annular cylindrical combustors with channel expansion [7]. For example, one wave ($n = 1$) rotating with respect to the inner diameter d_{c1} with a velocity $D = 1.11 \text{ km/s}$ was obtained in the PRC with $d_{c1} = 20 \text{ mm}$, $L_c = 10 \text{ mm}$, and specific flow rate $g_{\Sigma} = 132 \text{ kg}/(\text{s m}^2)$ [4]. In this work, five waves ($n = 5$) rotating with respect to the inner diameter d_{c1} with a velocity $D = 1.75 \text{ km/s}$ were obtained in the PRC with $d_{c1} = 100 \text{ mm}$, $L_c = 10 \text{ mm}$, and $g_{\Sigma} = 132 \text{ kg}/(\text{s m}^2)$. The scale effect in terms of the number of waves does exist ($n = 5 = 100 \text{ mm}/20 \text{ mm}$), but the TDW velocities are significantly different: The detonation velocity in the PRC with the greater diameter is appreciably higher. Obviously, the smaller the inner diameter of the PRC, the greater the influence of the centrifugal forces on the detonation products behind the TDW front for identical velocities of the products in the wave front. Therefore, the pressure of the detonation products behind the TDW front in the PRC with $d_{c1} = 20 \text{ mm}$ decreases more intensely and, hence, the TDW velocity decreases. The existence of a minimum PRC diameter $d_{c1\text{min}}$ at which CSD can still occur raises no doubts. Even for premixed and motionless mixtures, there exists a minimum diameter of the cylindrical surface around which the classical detonation wave can pass. It was demonstrated [15] that detonation propagation along a circular wall over a premixed mixture is possible if the condition $(d_{c1}/2) \geq 30b$

is satisfied (b is the longitudinal size of multifront detonation cells). The front moving along the wall has the radius $r_* = (3 \pm 1)b$; therefore, the wave structure is enlarged as the chemical activity of the mixture decreases (the parameter b increases), and the impulse loss behind the curved surface increases [16]. The detonation wave parameters decrease to a limit where the TDW cannot exist at all. For this reason, it was impossible to obtain CSD in the combustor with $d_{c1} = 20 \text{ mm}$ for a less chemically active mixture of methane and oxygen [7]. As the PRC diameter increases, the centrifugal forces acting on the products become less intense, and the CSD realization conditions approach those existing for the annular cylindrical combustor with channel expansion.

Manual and computer reconstructions of TDWs and the flow in their vicinity in the PRC plane and in the wave-fitted system for three TDWs are shown in Fig. 6. This reconstruction is based on the right-side fragment of the photographic records in Fig. 2b, which was scaled relative to the inner diameter of the combustor $d_{c1} = 100 \text{ mm}$.

It is seen that the manual and computer reconstruction are almost identical. To avoid too many details, Fig. 6a shows only contact line and one streamline passing through the front **BC**. The contact line near the PRC entrance is the boundary between the fresh mixture and products; further downstream, this line serves as the boundary between the layers of the detonation products. It is seen that the streamline crosses the waves many times (in the present case, four times). This is not good from the energy point of view because of the increase in the entropy of the products. Therefore, it is reasonable to reduce the PRC length without large changes in the detonation process. The TDWs were reconstructed manually in the following manner: The wave and flow elements on the circumferences of radii $r_{c1} \leq r \leq r_{c2}$ were shifted along these circumferences in proportion to the radius from the base radius passing through point **B**. For an identical angular velocity of wave rotation, the tangential velocity of the TDW segments increased from point

Fig. 6 Manual (a) and computer (b) reconstruction of TDWs and the flow in their vicinity in the PRC plane and in the wave-fitted system (see Fig. 2b)



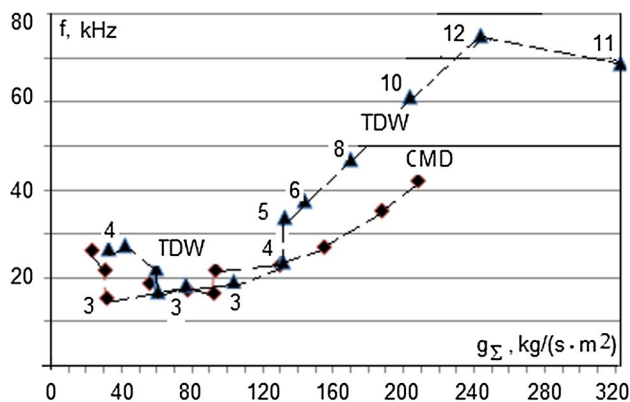


Fig. 7 TDW frequencies in the PRC for the CSD and CMD regimes; diamond symbol— $\Delta = 10$ mm, triangle symbol— $\Delta = 5$ mm; the numbers from 3 to 12 indicate the number of TDWs

B to point **D** in the proportion $D^1 = D \cdot r / r_{c1} = 1.93 \rightarrow 5.76$ km/s. As the normal component of the detonation velocity was constant for each point of the front **BC**, the TDW front was expected to deflect backward, which is observed in the reconstruction. The deflection for the points of the tail **CD** (shock wave in the products) is even more significant because the tail intensity decreases in the downstream direction. In annular cylindrical combustors with $L_c \approx 7 h$, the TDW tail at the combustor exit degenerates into an acoustic wave [6]. If the tail at point **D** in the PRC is also assumed to degenerate into an acoustic wave, then its velocity in the normal direction should be close to the velocity of sound in the products $D_n^1 = D \cdot (r_{c2} / r_{c1}) \cdot \sin \alpha \approx 1.3$ km/s [17], where $\alpha = 13^\circ$ is the angle between the tail and the tangential line to the circumference.

The TDW front height was measured on the basis of the photographic records. According to Fig. 6, the measured value of h is only the projection of the curved front **BC** onto the radius. Therefore, it becomes more and more different from the true size of the front **BC** as the number of waves decreases. This fact also offers an explanation to the variable value of the ratio h/l and its decrease with the decreasing number of TDWs.

The TDW frequencies in the PRC with $d_{c2} = 200$ mm and $\Delta = 5$ mm (CSD) and $\Delta = 10$ mm (CMD) are plotted in Fig. 7 as functions of the specific flow rate of the mixture g_Σ . There are only minor changes in the fuel-to-oxidizer equivalence ratio in the present case: $\phi = 0.85\text{--}1.08$.

For both combustors, the frequency of the rotating waves decreases with reduction in the specific flow rate of the mixture. It is only at small specific flow rates ($g_\Sigma = 30 \pm 10$ kg/(s m²)) that the TDWs degenerate into acoustic waves, and the number of TDWs increases from three to four. The CMD regime is observed in the interval $g_\Sigma = 208 \rightarrow 93$ kg/(s m²), and it transforms to the CSD regime as $g_\Sigma = 93 \rightarrow 23$ kg/(s m²). The mechanism of the

emergence and stable realization of the CMD regime and its transformation to the CSD regime was not clarified. It should be noted that the TDW velocities in all regimes stay within narrow limits $D = 2.0 \pm 0.2$ km/s despite wide-ranging changes in $\phi = 0.5\text{--}1.6$, respectively. This means that the flow gas dynamics produces a dominating effect on the process in this range of fuel-to-oxidizer equivalence ratio variation as compared to chemical physics in the detonation wave front. The imperfection of continuous detonation is estimated by the ratio $D/D_{CJ} = 0.6\text{--}0.8$, where D_{CJ} is the velocity of the ideal Chapman–Jouguet detonation for the present composition of the mixture. Smaller values of D/D_{CJ} correspond to greater values of ϕ .

5 Conclusions

1. Regimes of continuous spin detonation and continuous multifront detonation of a hydrogen–oxygen mixture were obtained in a plane-radial combustor with an inner diameter of 100 mm and exhaustion toward the periphery; CMD regimes were obtained for the first time.
2. It was demonstrated that CSD regimes have fuel-lean limits of existence in terms of the specific flow rate of the mixture for all geometric configurations of the combustor.
3. The structure of detonation waves was considered. For continuous spin detonation, the transverse detonation waves and the flow in the vicinity of these waves in the PRC plane were reconstructed. It was demonstrated that the detonation wave is significantly curved owing to the increase in the tangential component of the velocity along the combustor radius.
4. It was found that the scale effect is manifested only in terms of the number of rotating waves. However, the velocity of these waves increases with an increase in the PRC size because of the smaller influence of the centrifugal forces acting on the products and reducing the pressure behind the detonation front.
5. The velocity deficit of continuous spin detonation is 20–40% as compared to the velocity of the ideal Chapman–Jouguet detonation. (The smaller value corresponds to the fuel-lean mixture.)

Acknowledgements This work was supported by the Russian Foundation for Basic Research (Grant No. 18-41-540001r_a).

References

1. Voitsekhovskii, B.V.: Steady detonation. *Dokl. Akad. Nauk SSSR* **129**, 1254–1256 (1959)
2. Bykovskii, F.A., Vasil'ev, A.A., Vedernikov, E.F., Mitrofanov, V.V.: Explosive combustion of a gas mixture in radial annular chambers. *Combust. Explos. Shock Waves* **30**, 510–516 (1994). <https://doi.org/10.1007/BF00790158>
3. Bykovskii, F.A., Vedernikov, E.F.: Self-sustaining pulsating detonation of gas-mixture flow. *Combust. Explos. Shock Waves* **32**, 442–448 (1996). <https://doi.org/10.1007/BF01998496>
4. Bykovskii, F.A., Zhdan, S.A., Vedernikov, E.F., Samsonov, A.N., Misovets, O.V.: Continuous detonation of a hydrogen–oxygen mixture in a plane-radial combustor with exhaustion toward the periphery. Proceedings of XXXI All-Russia Conference “Siberian Thermophysical Workshop,” Nov 17–19, 2014, Novosibirsk, Russia, pp. 173–178
5. Tobita, A., Fujiwara, T., Wolanski, P.: Detonation engine and flying object provided therewith. U.S. Patent 7,784,267, issued August 31, 2010
6. Higashi, J., Ishiyama, C., Nakagami, S., et al.: Experimental study of disk-shaped rotating detonation turbine engine. 55th AIAA Aerospace Sciences Meeting, Grapevine, TX, AIAA Paper 2017-1286 (2017). <https://doi.org/10.2514/6.2017-1286>
7. Bykovskii, F.A., Zhdan, S.A.: Continuous spin detonation. *Izd. SO RAN, Novosibirsk* (2013)
8. Bykovskii, F.A., Vedernikov, E.F., Polozov, S.V., Golubev, Yu.V.: Initiation of detonation in flows of fuel-air mixtures. *Combust. Explos. Shock Waves* **43**, 345–354 (2007). <https://doi.org/10.1007/s10573-007-0048-8>
9. Bykovskii, F.A., Zhdan, S.A., Vedernikov, E.F.: Continuous detonation of methane/hydrogen–air mixtures in an annular cylindrical combustor. *Combust. Explos. Shock Waves* **54**, 472–481 (2018). <https://doi.org/10.1134/s0010508218040111>
10. Voitsekhovskii, B.V., Mitrofanov, V.V., Topchiyan, M.E.: Detonation front structure in gases. *Izd. Sib. Otd. Akad. Nauk SSSR, Novosibirsk* (1963)
11. Lewis, B., Elbe, G.: *Combustion, Flame, and Explosions of Gases*. Elsevier, New York (1961). <https://doi.org/10.1016/C2009-0-21751-X>
12. Nikolaev, YuA, Topchiyan, M.E.: Analysis of equilibrium flows in detonation waves in gases. *Combust. Explos. Shock Waves* **13**, 327–337 (1977). <https://doi.org/10.1007/BF00740309>
13. Nakagami, S., Matsuoka, K., Kasahara, J., Matsuo, A., Ikkoh, F.: Experimental study of the structure of forward-tilting rotating detonation waves and highly maintained combustion chamber pressure in disk-shaped combustor. *Proc. Combust. Inst.* **36**, 2673–2680 (2017). <https://doi.org/10.1016/j.proci.2016.07.097>
14. Bykovskii, F.A., Vedernikov, E.F.: Continuous detonation combustion of an annular gas-mixture layer. *Combust. Explos. Shock Waves* **32**, 489–491 (1996). <https://doi.org/10.1007/BF01998570>
15. Vasil'ev, A.A., Mitrofanov, V.V., Topchiyan, M.E.: Detonation waves in gases. *Combust. Explos. Shock Waves* **23**, 605–623 (1987). <https://doi.org/10.1007/BF00756541>
16. Mitrofanov, V.V.: Certain critical phenomena in detonation associated with momentum losses. *Combust. Explos. Shock Waves* **19**, 531–536 (1983). <https://doi.org/10.1007/BF00783670>
17. Deich, M.E.: *Technical Gas Dynamics*. Energiya, Moscow (1974)

Publisher's Note Springer Nature remains neutral with regard to jurisdictional claims in published maps and institutional affiliations.